



A high selectivity quaternized polysulfone membrane for alkaline direct methanol fuel cells



Graciela C. Abuin^a, Esteban A. Franceschini^b, Patrick Nonjola^c, Mkhulu K. Mathe^c, Mmalewane Modibedi^c, Horacio R. Corti^{b,*}

^a Centro de Procesos Superficiales, Instituto Nacional de Tecnología Industrial (INTI), Av. Gral. Paz 5445, B1650KNA, San Martín, Buenos Aires, Argentina

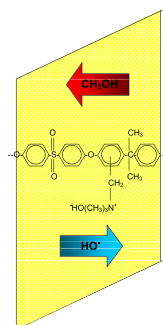
^b Departamento de Física de la Materia Condensada, Comisión Nacional de Energía Atómica (CNEA), Av. Gral. Paz 1499, B1650KNA, San Martín, Buenos Aires, Argentina

^c Council for Scientific & Industrial Research (CSIR), Material Science & Manufacturing, PO Box 395, Brumeria, Pretoria 0001, South Africa

HIGHLIGHTS

- Alkaline membranes were synthesized via quaternization of a commercial polysulfone.
- Young's modulus of QPAES membranes alkalized in 1 M KOH is similar to that of Nafion.
- Methanol permeability is much lower in QPAES than in Nafion membranes.
- Conductivities between 0.017 and 0.05 S cm⁻¹ were measured at 30 < T (°C) < 70 °C.
- Methanol selectivity of the QPAES membranes is higher than that of Nafion 117.

GRAPHICAL ABSTRACT



ARTICLE INFO

Article history:

Received 11 December 2014

Accepted 27 December 2014

Available online 30 December 2014

Keywords:

Polysulfone
Membranes
Alkaline
Fuel cells
Methanol

ABSTRACT

Alkaline membranes based on quaternized poly(arylene ether sulfone) (QPAES) were characterized in relation to their water and methanol uptake, methanol permeability, electrical conductivity, and mechanical properties. The performance of QPAES as electrolyte in alkaline direct methanol fuel cells was studied using a free-breathing single fuel cell at room temperature. Methanol uptake by QPAES membranes is lower than water, while their methanol permeability, determined in the temperature range from 30 °C to 75 °C, was much lower than for Nafion membranes. Young modulus of QPAES membranes decrease with the degree of alkalization of the membrane, although mechanical properties are still satisfactory for fuel cell applications for membrane alkalized with 2 M KOH, which additionally exhibit optimal hydroxide conductivity. Although the specific conductivity of QPAES membranes was lower than that reported for Nafion, its methanol selectivity (conductivity/methanol permeability ratio), is much higher than that reported for Nafion 117, and a commercial aminated polysulfone. In view of these results, QPAES membranes are expected to exhibit promising performance as an electrolyte in alkaline direct methanol fuel cells.

© 2014 Elsevier B.V. All rights reserved.

* Corresponding author.

E-mail address: hrcorti@cnea.gov.ar (H.R. Corti).

1. Introduction

Methanol economy has been proposed by Olah et al. [1] as a previous step to a future hydrogen economy, because methanol is the simplest, safest, and easiest way to store and transport hydrogen as a liquid hydrocarbon. A methanol-based economy involves not only the conversion of methanol to synthetic hydrocarbons and their products that are essential part of our life, but also its use as a fuel in internal combustion engines or methanol direct proton exchange membrane (PEM) fuel cells (DMFC).

The use of methanol instead of hydrogen for feeding PEM fuel cells for electric vehicle transportation would have the advantage of facilitating fuel distribution and on-board storage, leading to a higher autonomy. However, the large-scale deployment of DMFC will probably starts through its use as power source of portable electronics, due to a high theoretical power density as compared with Li-ion batteries [2,3].

The high methanol crossover through Nafion and inorganic- or organic-Nafion composite membranes reduces the efficiency of DMFC in comparison with hydrogen fed PEM fuel cells, [4–6] thus triggering the search for novel proton exchange membranes with reduced alcohol permeability. [7,8] Nevertheless, anion exchange membrane (AEM) direct methanol fuel cells have numerous advantages over proton exchange membrane DMFC. For example, non-noble and low cost metal, such as silver and nickel, can be used as electro-catalysts due to the inherently faster kinetics of oxygen reduction reaction in alkaline media. Furthermore, methanol oxidation is more facile in alkaline media than in acidic one [9–13].

Although the ionic conductivity of AEM is not as high as that of PEM membranes, [14,15] they have several advantages, namely: can be synthesized from low cost materials, and exhibit less alcohol crossover than PEM because the electro-osmotic transport of water and alcohol occurs from the cathode to the anode, that is, in opposite direction that solvent transport in PEM DMFC [16–18].

Several types of AEM have been developed during the last decade aiming to improve the performance of H_2/O_2 AEM fuel cells running with aqueous KOH electrolyte, first demonstrated by Bacon in the 1930s and used in the NASA missions two decades later. The polymeric materials currently under investigation for H_2/O_2 solid AEM fuel cells have been recently reviewed by Couture et al., [19] while their performance in direct alcohol AEM fuel cells was also analyzed [20,21].

Varcoe and coworkers were pioneers in synthesizing AEM with quaternized ammonium groups for DMFC by radiation grafting vinylbenzyl chloride (VBC) onto stable materials such as poly(ethylene-co-tetrafluoroethylene) (ETFE). [18,22] Other AEMs based on polymers containing a quaternary ammonium group have been developed and their electrical conductivity and methanol permeability have been reported, and in some cases they were tested in alcohol direct alkaline fuel cells (ADAFC). Among these quaternized membranes are: poly(ether sulfone cardo) (QPES-C), [23] poly(ether ketone cardo) (QPEK-C), [24] poly(phthalazinone ether sulfone ketone) (QPPEK), [16] poly(arylene ether sulfone) (QPAES), [12,25,26], QPAES cardo, [27] QPAES/crosslinked polyethylene, [28] and QPAES/ ZrO_2 composites, [29] poly(arylene ether) (QPAE), [30] poly(arylether oxadiazole) (QPAEO), [31] polystyrene-block-poly(ethylene-ran-butylene)-block-polystyrene (QSEBS), [32] poly(vinyl alcohol) (QPVA), [33] poly(vinyl chloride) (QPVC), [34] poly(vinylbenzyl chloride) (QPVBC), [35] and poly(vinylbenzyl chloride)-grafted-poly(ethylene-alt-tetrafluoroethylene) (QETFE-g-PVBC) [36].

C. C. Yang and coworkers and other authors have studied quaternized PVA (QPVA)-based membranes in relation to their methanol permeability and DMFC performance, including PVA cross-linked with sulfosuccinic acid (cPVA), [37] and composite

membranes of QPVA with SiO_2 , [38] quaternized SiO_2 , [39] Al_2O_3 , [40] chitosan, [41,42] and poly(epichlorohydrin) (PECH) [43].

Commercial AEM based on quaternary ammonium exchange groups have been developed by Tokuyama (Japan) on unknown backbone polymer (A201 membrane), by Solvay (Belgium) on cross-linked fluorinated polymer (Morgan ADP membrane), and by Fumatech (Germany) on polysulfones (FAA membrane). All of them have been tested in methanol and other ADAFC [44–54].

Membranes based on poly(arylene ether sulfone) with pendent quaternary ammonium (QPAES) have recently received much attention in relation to their use in solid-state alkaline fuel cell due to its relatively low cost and high electrical conductivity (up to $60\text{--}80\text{ mS cm}^{-1}$ at room temperature) [12,25]. Its high permselectivity is expected to be also useful for salinity gradient technologies, such as reverse electrodialysis. [55] Moreover, QPAES chemical stability seems to be compatible with the expected long operation lifetimes in alkaline fuel cell [56], and alkaline electrolyzer [57] applications.

The successful replacement of Nafion by quaternized AEM in DMFC strongly depend on the possibility of compensate the lower ion conductivity of the AEM with lower methanol permeability. In a previous work [12] we prepared a quaternized poly(arylene ether sulfone) membrane (QPAES) from a commercial polysulfone (Udel), quaternized by a trimethylamine treatment. The obtained AEMs exhibited good mechanical and conductivity, and sorbs more water but less methanol than Nafion over the whole range of water activities. Based on these results we claimed that QPAES membranes could exhibit promising barrier properties against methanol crossover in DMFC, although the permeability of methanol through these membranes was not studied.

In this work we determined the methanol permeability through QPAES membranes on a wide temperature range in order to confirm our expectations. We have also performed electrical conductivity measurements of QPAES membranes alkalized with 2.0 mol dm^{-3} KOH at temperatures up to 71°C , and the effect of the KOH concentration on the mechanical properties was evaluated using nanoindentation analysis to determine the Young's modulus of the AEMs. This parameter is related to the resistance of the material to be compressed, [58] which is relevant for fuel cell application. Finally, water and methanol uptake and partition coefficients were determined in bulky membranes, in order to compare with previous sorption results obtained using the quartz microbalance (QMB) technique on ultrathin (40 nm thickness) ones. [12] This analysis could help to decide whether the properties of bulky QPAES membranes differs from that of thin QPAES films, as those present in the three-phases region of the MEAs, as it was found in the case of Nafion [59].

In summary, the aim of this work is to characterize bulky QPAES membranes in order to obtain all the physico-chemical parameters needed for understanding the behavior of the membrane under direct methanol alkaline fuel cell conditions. These properties will be compared with those of Nafion® membrane properties, still the most used membrane in DMFC, and with those of a commercial alkaline membrane (A201®, Tokuyama).

2. Experimental

2.1. QPAES synthesis and membrane preparation

A commercial Udel® polysulfone was chloromethylated, ammoniated, and converted to the HO^- form, following a procedure described elsewhere. [12] Different KOH concentrations were used in order to analyze the effect of the HO^- counterion content on the membrane properties. Due to the Donnan equilibrium, the concentration of HO^- counterions in the membrane is that required to

compensate the positive charge of the quaternary ammonium groups on the polymer and the smaller concentration of K^+ coions. Both, the HO^- and K^+ concentration in the aqueous phase of the membrane increase with increasing KOH concentration of the external solution.

Nafion 117® membranes were pre-treated 1 h in 3 wt % H_2O_2 at 80 °C, rinsed 1 h in boiling water, converted to acid form by immersion during 1 h in 1 M H_2SO_4 at 80 °C, and rinsed again 1 h in boiling water.

The thicknesses of the membrane samples used in the conductivity and permeability measurements were determined by means of a micrometer Mahr XL1-57B-15 dead load gauge. In these cases the QPAES membranes, in HO^- form, were equilibrated in the corresponding solvent composition to obtain the swelled membrane thickness.

2.2. Characterization of the QPAES membranes

Water and methanol sorption, methanol partition coefficient, electrical conductivity, methanol permeability and elastic modulus were evaluated for the prepared QPAES membranes. Some of these properties were also determined for Nafion® (methanol permeability, Young's modulus) and the commercial alkaline membrane Tokuyama A201® (electrical conductivity) for comparative purposes.

2.2.1. Ionic exchange capacity

The ion exchange capacity (IEC) of QPAES membranes, alkalinized in 2 M KOH, was determined by acid–base titration of a membrane sample immersed in a known volume of 0.1 M HCl, and back titration of the final solution with 0.1 M NaOH.

2.2.2. Water sorption from the vapor

The isopiestic method was used for water uptake measurements from the vapor phase in bulky QPAES membranes (50 μm thickness), over the range of water activities from $a_w = 0.33$ to $a_w = 1$. Membrane samples, previously converted to the alkaline form by immersion in 2.0 mol dm^{-3} KOH, were maintained in isopiestic equilibrium at 30 °C in capped and sealed flasks, with the vapor phase of saturated solution of $MgCl_2 \cdot 6H_2O$ ($a_w = 0.33$), H_2SO_4 40.75 wt % ($a_w = 0.55$), saturated solution of NaCl ($a_w = 0.75$) and pure water ($a_w = 1$). Merck analytical grade chemicals as received and deionized water passed through a Millipore filter were employed.

Membrane samples were weighted daily until a constant mass of the wet membrane (m_t) was reached. Then, the samples were dried in oven at 130 °C up to constant weight (approximately 6 h) to determine dry membrane mass (m_0).

The water sorption of the membrane, expressed as the water mole number per mole of ionic group in the membrane, λ_w , at the water activity a_w is determined by the expression:

$$\lambda_w = \frac{(m_t - m_0)M_0}{m_0M_w} \quad (1)$$

where M_w is the water molecular mass (18.016 g mol^{-1}), and M_0 is the molar mass of the polymer per ionic group ($M_0 = IEC^{-1}$).

2.2.3. Water and methanol sorption from the liquid

Sorption of methanol and water/methanol mixtures from the liquid phase were also measured in bulky QPAES membranes, in the HO^- form, equilibrated around 15 days at room temperature with aqueous methanol solutions containing 20, 60 and 80 wt% of methanol, and in pure methanol, corresponding to methanol activities (a_m) 0.19, 0.56, 0.73 and 1.0, respectively. After this treatment the concentration of HO^- counterions in the membrane is

equal to the concentration of quaternary ammonium groups, due to the lack of K^+ coions in the membrane. The mass of wet membranes (with water and methanol uptake), m_t , was determined after a constant weight of the samples was reached for at least three days.

The methanol and water contributions to the liquid sorption by the membranes were determined by re-immersing them during 24 h in a covered flask containing a volume of pure water, enough to transfer all methanol sorbed by membrane to the liquid phase. From the concentration of methanol in the liquid solution, measured by gas chromatography, we calculate the mass of methanol inside the membrane, m_m . Then, the membrane samples were dried in oven at 130 °C up to constant weight (approximately 6 h) to determine the dry membrane mass, m_0 . Therefore we calculated the mass of sorbed water as: $m_w = m_t - m_m - m_0$. The methanol sorption of the membrane, expressed as the methanol mole number per mole of ionic group in the membrane, λ_m , at the methanol molar fraction (x_m) is expressed as:

$$\lambda_m = \frac{m_m M_0}{m_0 M_m} \quad (2)$$

where M_m is the methanol molecular mass (32.042 g mol^{-1}). The total liquid sorption of the membranes, λ_{w+m} , defined as the sum of λ_w and λ_m , was also determined.

2.2.4. Conductivity measurements

The electrical conductivity of QPAES membranes, converted to HO^- form by immersion in 2 M KOH solution overnight and equilibrated in pure water vapor ($a_w = 1$) previously to the conductivity measurements, was measured with the AC impedance technique with a four electrodes cell, as shown in Fig. 1. A membrane sample (1), 3 cm \times 1 cm, was placed in contact with the four electrodes (2): two platinum foils separated 3 cm (A and D), and two inner platinum wires (B and C) separated 1 cm, which were supported on a Teflon plate. The membrane was sandwiched by a second Teflon plate (3) having slots (4) to allow membrane hydration. Finally two steel plates (5) were placed and fixed with screws (6) that were adjusted with a torque of 0.5 kg cm to ensure good contact between the membrane and the electrodes.

The impedance measurements were made in the frequency range between 1 Hz and 100 kHz, with an amplitude of $\pm 10 \mu A$,

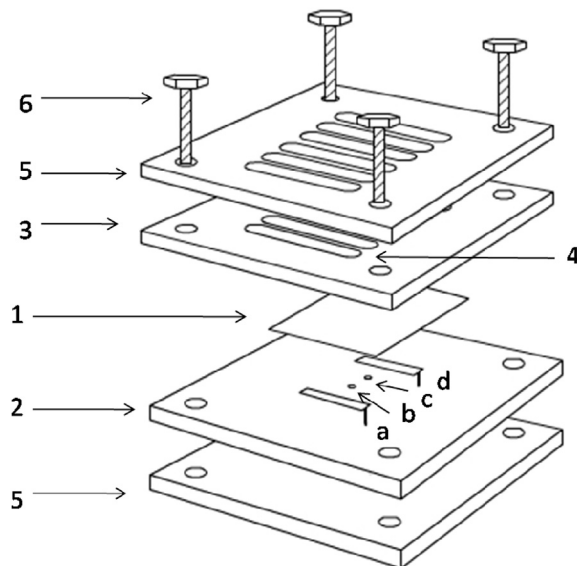


Fig. 1. Scheme of the 4-electrodes cell for conductivity measurements. The meaning of the labels are explained in the text.

using an AutoLab PGSTAT 302N coupled to a Frequency Response Analyzer (FRA). The specific longitudinal conductivity, σ , of the membrane in the was calculated as:

$$\sigma = \frac{l}{R\delta a} \quad (3)$$

where R is the electric resistance of the membrane, obtained from the intersection with the real axis of the Nyquist impedance diagram, l is the distance between the inner electrodes, δ and a are the thickness and width of the membrane, respectively, measured in the swelled state. The product δa represents the cross sectional area of the membrane.

2.2.5. Methanol permeability

Methanol permeability was measured by a procedure described in detail elsewhere, using a two-chamber diffusion technique [8]. Both chambers have a volume of 11.3 cm³ and they are separated by the membrane sample, whose exposed area, A , is 3.14 cm². Two Teflon o-rings and two stainless steel meshes fix the membranes in the cell to avoid deformation by uncompensated pressures between both chambers during the experiment. The QPAES membranes were converted to HO[−] form by immersion in 2 M KOH solution overnight and equilibrated in pure water vapor ($a_w = 1$) previously to the permeability measurements.

The donor chamber is fed with a methanol solution 20 w%, and the receptor chamber with pure water, both at a flow rate of 1 cm³ min^{−1} (using two Gilson 305 HPLC pumps). Both, the aqueous methanol and the pure water are discarded in order to keep a constant concentration in the donor chamber and to establish a stationary methanol concentration gradient through the membrane. Before entering the permeation cell, a pre-heater raises the temperature of the fluids close to the working temperature, while the temperature of the permeation cell is controlled at ± 1 K.

After ≈ 1 h water is re-circulated ($t = 0$) through the receptor loop, which includes a calibrated vibrating tube densimeter thermostated at 25 °C. The increase of methanol concentration with time in the receptor chamber is determined by the decreases of the density of the methanol aqueous solution. Thus, the methanol permeability, P , through the membrane can be obtained by the following expression [8]:

$$\ln\left(1 - \frac{c_R(t)}{c_D}\right) = -\frac{AP}{V_R l} t \quad (4)$$

where c_D and $c_R(t)$ are the constant and time dependent methanol concentrations in the donor and receptor chambers, respectively, V_R is the total receptor loop volume, and l is the membrane thickness, measured in the swelled state.

If the water counterflow due to the gradient of water concentration opposite to the gradient of methanol concentration turns to be important, we would observe a deviation of the linear plot $\ln(1 - c_R(t)/c_D)$ vs. t at long times, a fact that has not been detected in our permeability measurements. Even considering that the linearity is preserved due to a compensation of effects (i.e. changes in density), it should be noted that diffusion coefficients, and consequently permeability coefficients, are magnitudes that depend on the adopted reference system to measure the flows. By referring the methanol flow to the membrane (a Hittorf-like reference system) we do not need to correct methanol flow by the associated water flow, as in the case of using the Fick's reference system.

2.2.6. Methanol partition and diffusion coefficients

The methanol permeation, P , between two solutions separated by a membrane is related to the diffusion coefficient inside the

membrane, D , according to the simple relationship:

$$P = DK \quad (5)$$

where K is the methanol partition coefficient, that is, the ratio between the methanol concentrations in the membrane and the solution phases. Thus, the methanol crossover through PEM or AEM membranes used in DMFC is determined not only by the methanol mobility inside the membrane, but also by the capacity of the membrane to sorb (dissolve) methanol.

For membranes equilibrated with a pure solvent (water or methanol), the solvent uptake from the liquid is a measured of K . However, the methanol (or water) partition coefficient in membranes equilibrated with methanol–water mixtures is not commonly reported, and the relationship between permeability and sorption is not well defined.

In this work we determined the partition coefficient of methanol in QPAES membranes equilibrated with an aqueous methanol solution at the concentration used in the permeability experiments (20 w%, or $x_m = 0.12$, or $a_m = 0.19$) by extraction in heavy water (D₂O, 99.97%) followed by ¹H NMR measurement of water and methanol. This method has the advantage of eliminating errors in the measurement of m_w by differences of masses as in the method described in Section 2.2.3.

In this method a QPAES membrane is equilibrated with the aqueous methanol solution, then removed from the solution, dried superficially with tissue paper, introduced into a small vial containing a known mass (around 2 g) of D₂O (99.97 wt%) and 100 mg of Na₂CH₃COO (Carlo Erba, analytical grade) used as a reference, and the vial was immediately sealed. A nitrogen flow was maintained during this procedure in order to avoid contamination of D₂O with water.

After several days of equilibration, water and methanol originally sorbed in the membrane was transferred to the D₂O phase, and their concentrations were determined by analyzing the ¹H-RMN spectra, using a Bruker Avance II 500 NMR spectrometer at 500.13 MHz, with full ¹³C decoupling. The integrated areas of methanol and water peaks were compared to that of sodium acetate used as a reference. Finally, the dry mass of the membrane was determined by desorbing the D₂O in an oven at 130 °C.

From the measured masses of methanol (m_m) and water (m_w) uptaken by the membrane, and the methanol composition of equilibration solution expressed as methanol mass fraction (χ_m), the methanol partition coefficient in mass basis, K , can be calculated as:

$$K = \frac{m_m}{\chi_m(m_m + m_w)} \quad (6)$$

where, in this case, $\chi_m = 0.20$.

2.2.7. Mechanical properties

A Multimode Nanoscope IIIa AFM (Bruker) was employed for the study of the mechanical properties of the QPAES membranes. The system was equipped with 150 μ m lateral scan range and a 5 μ m z-scanner. Si₃N₄ tips with a spring constant $k = 0.48$ – 0.52 N m^{−1} were used for the elasticity measurements (Nano Devices, Veeco Metrology, Santa Barbara, California, pyramidal tip shape, cone half angle $\alpha = 18^\circ$, tip curvature radius $r < 10$ nm, resonant frequency nominal: 54 kHz, measured: 47.60 kHz). The spring constant was measured for each tip before and after of the measurements, using the Nanoscope Software 5.34 Rev. 2004.

The indentation of an AFM tip into a soft sample can be modeled using Hertzian contact mechanics. [60] This theory provides a direct approach to the material elasticity for a sample with a semi-

infinite thickness. The expression for the force curve on an elastic sample is given in terms of the properties of the tip (k , α), Young's modulus (E), and Poisson's ratio (ν): [61].

$$\delta(z) = -(z - z_0) + \frac{a}{K} - \left[\left(\frac{a}{K} \right)^2 - \frac{2a}{K} (z - z_0) \right]^{1/2} \quad (7)$$

where $\delta(z)$ is the indentation, z is the piezo position at all time, z_0 is the piezo position when the tip hits the sample (contact point), $K = E/(1 - \nu^2)$, and $a = (k/\pi \tan \alpha)$. The loading force on the sample is $F(z) = k\delta(z)$, Young's modulus is obtained by fitting the corresponding $F(z)$ vs. z or $\delta(z)$ vs. z curves fixing $\nu = 0.5$ (elastic samples).

The procedure to obtain the force curves has been described in detail elsewhere [61]. Indentation measurements were carried out in membranes immersed in water in order to analyze the response of the hydrated membranes, in conditions similar to that found under fuel cells operation. The indentation depths were shorter than 120 nm and several indentation curves were obtained for each membranes in different points separated few microns.

2.2.8. Single cell test

The membrane-electrode assembly for DMFC testing was fabricated as follows: the catalytic ink was prepared by sonicating the catalytic powder (Pt/C was used as anodic and cathodic catalysts) 60 wt% in ethanol with 5 wt% of a binder, consisting of QPAES polymer dissolved in DMF/ethanol solution. The inks were applied on carbon paper (TGPH030) using the air-brush method to form anode and cathode layers. The metal loading was 3.2 and 2.2 mg Pt cm⁻² in the cathode an anode, respectively. The anode and cathode layers were hot pressed onto the membrane (previously soaked in 3 M KOH during 4 h) at 100 °C and 2 bars for 3 min.

Alkaline DMFC performance was evaluated under passive conditions in a single fuel cell (Heliocentris) at room temperature (25 °C) and ambient air (free-breathing). Aqueous solutions containing 3 M methanol and OKH between 1 M and 5 M were used as fuel. The geometric area of the electrode was 9.0 cm². The fuel (18 cm³) was poured into a reservoir attached to the anode side. The fuel was allowed to diffuse into the anode catalyst layer driven by the concentration gradient set between the reservoir and the anode. Anode and cathode stainless steel plates with pin-holes served as current collectors. Current–voltage curves were recorded galvanostatically using a two-electrode set-up by means of an AutoLab PGSTAT 302.

3. Results and discussion

3.1. Ionic exchange capacity

Ionic Exchange capacity (IEC) of the QPAES membrane alkalinized in 2 M KOH was 0.80 ± 0.05 mmol g⁻¹ compared with IEC = 1.94 mmol g⁻¹ for a completely chloromethylated and quaternized polymer. Wang et al. [62] observed that the chloromethylation is the more difficult step to control during the polymer synthesis, which could result in a low amount of chloromethyl groups attached to the polymer. In this case we decided to prepare a polymer with lower IEC than that prepared in a previous study [12] with the purpose of increasing the methanol barrier properties of the membrane, although the ionic conductivity of the membrane could be depressed.

3.2. Water–methanol uptake and partition constant

Table 1 shows methanol and water sorption results in bulky

QPAES measured from the liquid phase at room temperature, using the immersion method membranes along with the partition coefficient calculated with equation (6). As can be seen in Table 1, methanol partition coefficients in QPAES membranes, in the methanol concentration range from $x_m = 0.12$ to 0.69, are nearly constant ($K = 1.17 \pm 0.05$), and are similar to that measured in Nafion® membranes. [8].

Water sorption from the vapor phase in bulky QPAES membranes alkalinized in 2 M KOH (50 μm thickness) is showed in Fig. 2, compared with results in Nafion® membranes. [63] Water uptake results from our previous works [12,59] measured in an ultrathin QPAES and Nafion membranes by the QMB technique are also included in Fig. 2. This measurement are inspired in the fact that membrane polymer is present as a 5–100 nm thin film surrounding catalyst particles in membrane fuel cell threephase region. In this geometry, the properties of the material may differ significantly from those in bulk membranes and the characterization polymer thin film structure and transport behavior is critical.

Comparison between water uptake in bulky QPAES and Nafion membranes show that at $a_w > 0.8$ is water sorption in QPAES membranes higher than in Nafion® ones. The behavior changes at $a_w < 0.8$, being water sorption in bulky QPAES membranes lower than that of Nafion® ones.

As it can be seen in Fig. 2 and was discussed in our previous work [59], the 2D confinement of Nafion thin film casted over the Au electrode of the QMB quartz crystal, restricts the swelling in the out-of-plane direction, and this could be the reason for the lower water sorption observed in our thin Nafion films compared to the bulky unsupported membranes. On the contrary, by comparing results of water uptake in bulky QPAES membranes and a 40 nm QPAES membrane over the Au substrate, it is found that the sorption behavior is similar in both bulky and ultra-thin PSQ membranes.

In Fig. 3 it is shown the methanol sorption in bulky QPAES membranes from the liquid phase along with methanol uptake of an ultrathin QPAES from the pure methanol vapor phase reported in our previous work [12]. It can be seen that pure methanol sorption values in bulky QPAES membranes are higher than that of the ultrathin one.

3.3. Electrical conductivity

The QPAES membranes were converted to HO⁻ form by immersion in 2 M KOH solution overnight and equilibrated in pure water vapor ($a_w = 1$) previously to the conductivity measurements, performed in the temperature range from 30 °C to 71 °C. The conductivities were determined in water in order to compare them with the results reported in the literature for QPAES membranes. The presence of methanol in AEM membranes for alkaline DMFC will decrease the conductivity because of the lower swelling (see Table 1). However, at the typical concentrations used in DMFC (up to 3 M or $x_m \approx 0.05$), the swelling effect on the membrane conductivity is expected to be moderated.

Tokuyama A201 membrane, having 30 μm thickness and IEC = 1.7 mmol g⁻¹ (according to the data provided by the

Table 1
Water and methanol sorption from liquid mixtures and partition coefficient for bulky QPAES membrane at ambient temperature.

x_m	λ_w	λ_m	λ_{w+m}	K
0.00	17.3 ± 1.0	0.0	17.3 ± 1.0	
0.12	9.4 ± 0.6	1.6 ± 0.1	11.0 ± 0.6	1.14
0.46	3.2 ± 0.2	4.1 ± 0.2	7.3 ± 0.3	1.16
0.69	0.3 ± 0.1	5.5 ± 0.3	5.8 ± 0.3	1.22
1.00	0.0	6.2 ± 0.4	6.2 ± 0.4	

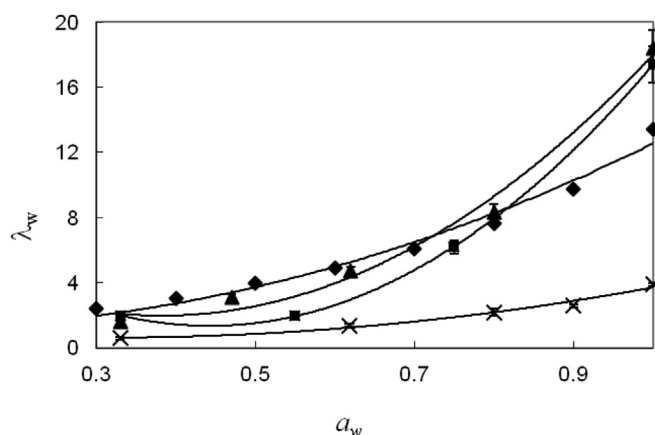


Fig. 2. Water sorption of (■) bulky QPAES membrane, (◆) bulky Nafion® membrane [62], (▲) 40 nm QPAES membrane [12] and (x) 27–62 nm Nafion® membrane cast over Au [59], measured at room temperature.

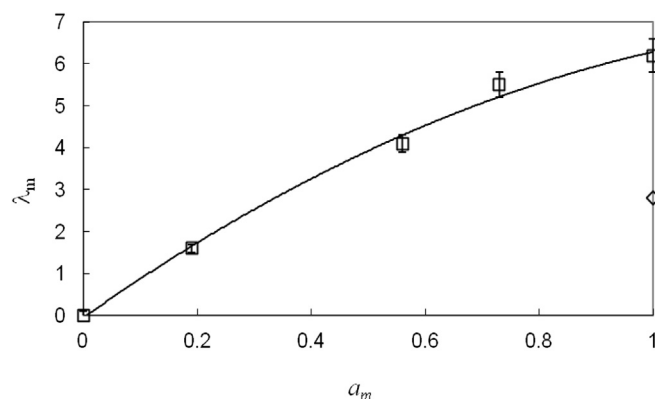


Fig. 3. Methanol sorption of (□) bulky QPAES membrane, (◇) 40 nm QPAES [21] measured at room temperature.

manufacturer), was measured in the same conditions with comparative purposes. The conductivity results for these membranes are shown in Fig. 4, along with those reported by Rao et al. [26] and Wang et al. [62] for QPAES membranes with similar structure.

It is important to emphasize that the conductivity is mainly due to the HO^- counterions in the membrane, because the ionic mobility of the positive ammonium groups attached to the polymer chain is very low, and the K^+ coions concentration is expected to be limited by Donnan exclusion. Therefore, when comparing the conductivities of anion exchange membranes, the IEC becomes the key parameter, provided that the membranes were previously equilibrated in the same solvent and alkali concentration.

QPAES membranes synthesized by Rao et al. [26] have $\text{IEC} = 1.20 \text{ mmol g}^{-1}$, which is higher than the IEC of our membranes. Wang et al. [62] prepared chloromethylated polysulfone (CMPS) membranes quaternized by two routes: with ternary amines (including trimethylamine, TMA) of a casted CMPS membrane, following a procedure identical to that used in this work; ii) adding tetramethyl ethylene diamine (TMEDA) to the casting solution of the chloromethylated polysulfone polymer. In the last case the authors achieved a higher quaternization (2 chloromethyl groups per repeating unit), and the IEC (not reported) is supposed to be higher than that of our membranes.

The conductivity at 25 °C of our QPAES membrane quaternized with TMA, is higher than that reported by Wang et al. [62], although

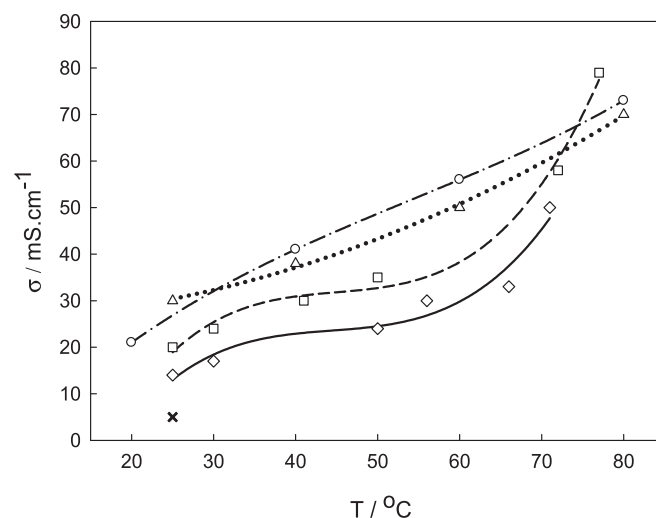


Fig. 4. Specific electrical conductivities of: (◇) QPAES – this work; (□) Tokuyama A201; (○) QPAES [26]; (x) QPAES-TMA [62]; (Δ) QPAES-TMEDA [62].

is lower than that reported for the QPAES membrane quaternized with TMEDA in the 30 °C–80 °C temperature range, and also lower than the measured for the commercial A201® membrane by Tokuyama. The general pattern observed for the conductivity of these membranes seems to be dominated by the IEC, although the water uptake restriction imposed by crosslinking could also have an important role.

Zhao et al. [25] have synthesized poly (arylene ether sulfone)s with 1,1,2,3,3-pentamethylguanidine exchange group by copolymerization of bis(4-chlorophenyl sulfone) and bisphenol. The resulting polymers have different proportions of the hydrophilic and hydrophobic components and, except for a particular composition with high conductivity, the prepared membranes have conductivities from 10 to 25 mS cm^{-1} at 30 °C up to 30–40 mS cm^{-1} at 80 °C, that is, close to those reported in this work (not shown in Fig. 4).

Li et al. [29,30] synthesized poly(arylene ether sulfone)s containing tetraphenyl methane moieties, with IEC between 0.41 and 2.38 mmol g^{-1} . The authors found that the electrical conductivity increase from 1.2 up to 25 mS cm^{-1} at 20 °C with increasing IEC.

The low conductivity of our partially ammoniated ($\text{IEC} = 0.80 \text{ mmol g}^{-1}$) membrane (14 mS cm^{-1} at 20 °C) as

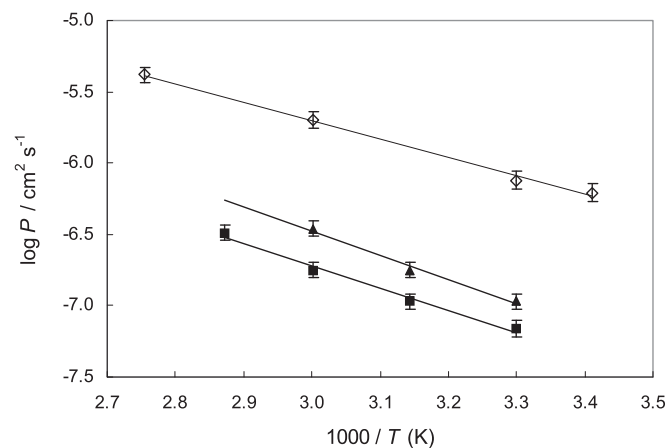


Fig. 5. Temperature dependence of the methanol permeability of QPAES and Nafion® membranes, methanol concentration 20% w/w. (■) QPAES alkalinized with 1 M KOH; (▲) QPAES alkalinized with 2 M KOH; (◇) Nafion 117®.

compared with that prepared previously (83.3 mS cm^{-1} at 20°C), measured after alkalization in 2 M KOH, is certainly related to its lower IEC, as mentioned in Section 3.1. Consequently, a comparative analysis of our membranes with different QPAES membranes reported in the literature is not complete until the effect of the low IEC on the methanol barrier properties is discussed. As we will see in the next section the reduced IEC leads to a low methanol permeability, which in turns determines the high methanol selectivity of the membrane.

3.4. Methanol permeability measurements

The permeability and diffusion coefficients of methanol in QPAES membranes have not been previously reported in the literature. Fig. 5 shows the methanol permeability measured in a QPAES membrane alkalized at different KOH concentrations. Methanol permeation was measured at temperatures from 30°C to 75°C . For comparison, the methanol permeability data for Nafion® membranes are also shown in Fig. 5.

Table 2 shows the permeability coefficient of methanol through the membrane and the calculated diffusion coefficient (from equation (5)) for QPAES membranes alkalized in 1 M KOH, using the partition coefficient determined in Table 1 at 25°C and $x_m = 0.12$, assuming it remains constant between 25°C and 30°C .

It is observed that the QPAES membrane methanol permeability is much lower than that reported for Nafion 117® membranes. Furthermore, methanol permeability increases with the KOH concentration used for equilibration, probably due to polymer deterioration related with the alkali effect over the poly(arylene ether sulfone) chain [16].

The apparent activation energy of the methanol permeation were 29.9 kJ mol^{-1} and 32.7 kJ mol^{-1} for QPAES membranes alkalized with 1 and 2 M KOH, respectively; being these values higher than that obtained for Nafion® (25.2 kJ mol^{-1}). The results indicate that the QPAES membranes exhibit a high barrier to methanol crossover, therefore it could improve the efficiency of DMFC. It is well-known that the effect of methanol crossover in AEM is much lower than in DMFC using PEM, such as Nafion. The electroosmotic drag of methanol in AEM is in opposite direction because the current in the membranes is driven by HO^- ions, while in Nafion is driven by H^+ , which enhance the methanol crossover from anode to cathode.

3.5. Mechanical properties

Fig. 6 shows typical indentation curves in the approach direction for QPAES membranes alkalized at different KOH concentrations (1–2.5 M). Since the main goal of these measurements was to determine the effect of the KOH doping on the mechanical integrity of the membranes, we have performed this measurements with membranes equilibrated in aqueous KOH solutions. Young's module of membranes immersed in methanol–water is expected to decrease with the methanol content because the swelling is lower in methanol-rich solutions.

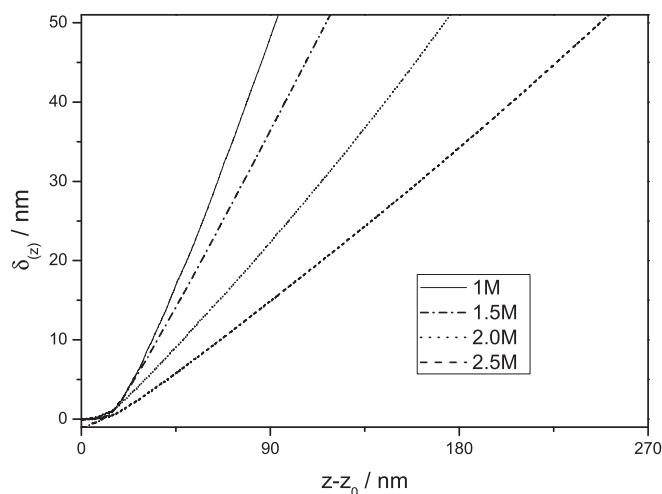


Fig. 6. Indentation curves on the QPAES membranes surface doped with different KOH concentrations.

The mechanical contact model [60] fits satisfactorily the experimental data by adjusting the value of the Young's modulus (E). Neither, structural breakdowns, nor inelastic deformations appear during the indentation, as revealed by the smooth extension (and retraction) curves obtained, indicating that the sample has a purely elastic response.

The measured Young's module for QPAES membranes, obtained by averaging around 30 curves obtained by indentation in different points of membrane surface, are shown in Table 3. The Young modulus for the membrane alkalized in 1 M KOH is similar to that reported for Nafion (90–290 MPa), [12,64] but decreases significantly when the membrane is alkalized in more concentrated KOH solutions. It is worthy note that the Young's modulus observed for membranes in 2 M KOH (10 MPa) is still compatible with its use in fuel cells. Rao et al. [26] reported Young's modulus of 1.46 GPa for QPAES membranes but the measurements were performed at 50% relative humidity and the alkaline concentration used was not indicated. Similarly, Zhang et al. [27] obtained Young's modulus of 1.09–1.94 GPa for QPAES cardo membranes at 30% relative humidity.

Mechanical properties for different types of polysulfone membranes have been previously reported. For instance, Ates et al. [65] measured Young's modulus as low as 0.15–0.5 MPa for 3-phenyl-3,4-dihydro-1,3-benzoxazine and polysulfones with benzoxazine end groups membranes, while Di Vona et al. [66] measured Young's modulus of 540–2950 MPa for sulfonated polyphenylsulfone membranes with different thermal treatments.

For QPAES, different authors [27,29,67] have reported tensile strength in the range 25–60 MPa and elongation at break between 6 and 19%. It is worthy to note that mechanical properties obtained from the tensile strength technique are not comparable with those obtained by nanoindentation because they correspond to different types of material deformation (stretching and compression,

Table 2
Methanol permeability and diffusion coefficient of QPAES membranes.

T ($^\circ\text{C}$)	$P/10^7 \text{ cm}^2 \text{ s}^{-1}$ (1 M KOH)	$P/10^7 \text{ cm}^2 \text{ s}^{-1}$ (2 M KOH)	$D/10^8 \text{ cm}^2 \text{ s}^{-1}$ (1 M KOH)
30	0.76 ± 0.07	1.14 ± 0.07	6.7 ± 0.6^a
45	1.19 ± 0.13	1.90 ± 0.12	—
60	2.01 ± 0.22	3.70 ± 0.23	—
75	3.54 ± 0.32	—	—

^a Calculated with $K = 1.14$.

Table 3
Young's modulus of hydrated QPAES membranes alkalized in KOH solutions.

KOH molarity	E/MPa
1.0	250 ± 7
1.5	50 ± 5.5
2.0	10 ± 0.9
2.5	5 ± 0.4

respectively).

3.6. Membrane performance in a passive alkaline DMFC

In Fig. 7 are summarized the polarization curves and power density plots for the MEA prepared with the QPAES membrane and Pt/C catalyst on the anode and cathode sides. It is observed that the performance improve as the KOH concentration increase from 1 M to 3 M, although decrease slightly as the KOH concentration raises to 5 M. This behavior is expected on the basis of the low permeability of methanol through QPAES.

It is worth to note that, after preconditioning the cell in 3 M $\text{CH}_3\text{OH} + 1 \text{ M KOH}$ during 12 h, the power density increase by a factor two, probably because of the slow accessibility of methanol to the three-phases region under passive conditions.

The relatively low power density of the single cell can be due to several factors: the low working temperature, the use of Pt/C in the anode (a bimetallic Pt–Ru/C catalyst would yield higher efficiency for the methanol oxidation reaction), and the high resistivity of the assembly (a disadvantage that can be avoided by using thinner membranes). A common drawback for alkaline DMFCs is the formation of carbonates when the methanol oxidation proceeds toward CO_2 formation. In passive fuel cells this could lead to a dramatic reduction of the efficiency due to the decrease of conductivity of the AEM. However, it is probably that methanol oxidation in our cell yields to intermediate oxidation products, such as formic acid, instead of CO_2 . A detailed study of the electro-oxidation products in the alkaline DMFC is needed to determine the best conditions to avoid carbonate formation. A compromise between a loss of electrochemical efficiency due to incomplete methanol oxidation, and enhanced mass and charge transfer in the catalytic layer and membrane due to non-gaseous products is crucial.

3.7. Feasibility of QPAES membranes for alkaline DMFC

In a previous work [12] we found a maximum HO^- conductivity in the QPAES membranes doped in KOH 2 M. These results are

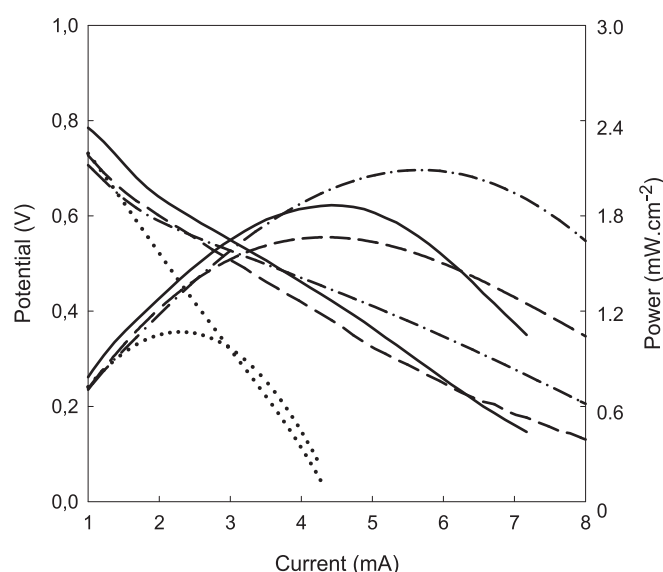


Fig. 7. Single cell performance at 25 °C in a passive DMFC running with 3 M CH_3OH with 1 M KOH (dotted lines), 3 M KOH (solid lines), 5 M KOH (dashed lines). The performance with 3 M $\text{CH}_3\text{OH} + 1 \text{ M KOH}$ after 12 h of preconditioning is displayed with dot-dashed lines.

consistent with those found by Fang et al. [17], who proposed that the depletion in the conductivity of quaternized poly(phthalazinon ether sulfone) membranes can be due to the displacement of the ammonium group by HO^- via a nucleophilic displacement reaction. This alkali effect can also explain the decrease in the Young's modulus at high KOH concentrations and the higher methanol permeation coefficient observed for membranes equilibrated with high concentration KOH solutions.

In summary, the whole picture that emerges from our characterization of the QPAES membranes with a moderated IEC is that conductivity is the highest for membranes alkalinized with 2 M KOH, while the mechanical properties and methanol permeability are much better for membranes alkalinized in 1 M KOH. Therefore, a criterion should be adopted to decide what properties of the AEM are more important in relation to its use in DMFC.

Alcohol crossover and cell electrical resistance are the relevant properties for DMFC performance, which are closely related to the membrane used in the preparation of the membrane-electrode assembly (MEA). Although mechanical properties, as well as the chemical and thermal stability of the membrane, could also be important when durability is considered, the membrane selectivity, β , defined by Pivovar et al. [68] as the ratio between the ion conductivity and permeability of the membrane,

$$\beta = \frac{\sigma}{P} \quad (8)$$

is the best indicator of the membrane feasibility for use in DMFC.

For Nafion 117 membranes we have measured conductivities of 0.092 S cm^{-1} and 0.189 S cm^{-1} , while the methanol permeability was $1.25 \cdot 10^{-6} \text{ cm}^2 \text{ s}^{-1}$ and $2.66 \cdot 10^{-6} \text{ cm}^2 \text{ s}^{-1}$ at 30 and 60 °C, respectively. [8] The selectivities of QPAES at 30 °C and 60 °C calculated with the results reported in this work are summarized in Table 4, along with those for Nafion and for the QPAES membranes studied by Jung et al. [28] by casting (C) and pore-filling (PF) of polyethylene membranes with a commercial aminated polysulfone. The chemical structure of this aminated polysulfone is compared with our QPAES in Fig. 8.

The results in Table 4 indicate that the selectivity of the QPAES membranes prepared in this work is higher than that of Nafion 117 in the temperature range of interest for DMFC. Evidently, the low conductivity of our QPAES membranes due to the moderate IEC is compensated by a higher barrier to methanol as compared to Nafion. Moreover, the membranes prepared in this work exhibit selectivities between 5 and 10 times higher as compared with membranes prepared by casting and pore-filling from a commercial QPAES [28].

It is worth mention that the high conductivity QPAES membrane with pentamethyl-guanidine groups, recently prepared by Zhao et al. [25], exhibit a very low methanol permeability ($1\text{--}10 \cdot 10^{-9} \text{ cm}^2 \text{ s}^{-1}$), which would result in selectivities 50–100 times higher than those found for our membranes. These authors measured the methanol permeability after vacuum drying the membranes at 60 and 120 °C for several hours, although the same treatment was apparently not applied to the membranes used in

Table 4
Selectivities (in S s cm^{-3}) of QPAES and Nafion membranes.

Membrane	β (30 °C)	β (60 °C)	Reference
Nafion	7.4×10^4	7.1×10^4	[8]
QPAES	1.5×10^5	8.9×10^4	This work
QPAES ^a	$0.5\text{--}1.1 \times 10^4$ (C)		[28]
	$2.3\text{--}2.8 \times 10^4$ (PF)		

^a Measured at 25 °C.

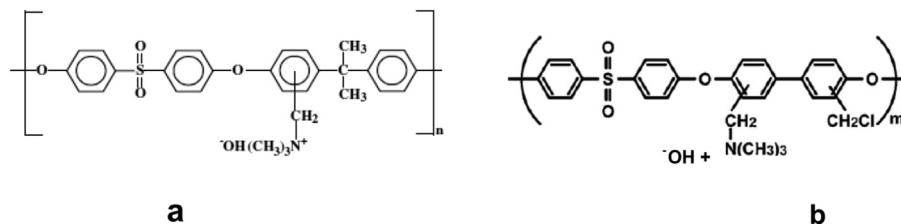


Fig. 8. Structure of the QPAES: (a) prepared in this work; (b) commercial aminated Asahi polysulfone [28].

the conductivity measurements. Thus, the huge selectivity calculated from these data (not reported by the authors), could not be reliable.

Very recently new anion and proton exchange membranes have been proposed for direct methanol fuel cells with special emphasis in their selectivities. Rao et al. [69] synthesized a series of phenolphthalein-based cardo poly(arylene ether sulfone) block copolymers containing imidazolium group which exhibit selectivities in the range $(3.7\text{--}4.7) \cdot 10^5 \text{ S s cm}^{-3}$ at 20°C . According to the authors, these membranes have the highest selectivity reported for AEM, and they are close to that found for our QPAES membranes. On the other hand, Wei et al. [70], prepared non-fluorinated PEM via the in-situ grafting of sodium 4-styrene sulfonate (NaSS) to hydrogenated nitrile butadiene rubber (HNBR), obtaining membranes whose conductivities and methanol permeabilities depend on the NaSS content. However, the measured selectivities are lower or close to the selectivity of a Nafion 212 membrane $(4.10^4 \text{ S s cm}^{-3})$ with a proton conductivity one order of magnitude lower than Nafion.

Thus, while the selectivity of PEM for DMFC rarely improve the performance of Nafion membranes, the QPAES membranes reported in this work and other AEMs can achieve much higher selectivity than the expensive Nafion membranes.

4. Conclusions

QPAES was synthesized via modification and subsequent quaternization of Udel® commercial polysulfone. The ionomer was used to prepare membranes which exhibit promising properties for application as AEM membranes in alkaline direct methanol fuel cells due to the following features: i) methanol permeability is much lower than in Nafion membranes over the temperature range $30^\circ\text{C}\text{--}75^\circ\text{C}$; ii) Young modulus is similar than those observed in Nafion for membranes alkalized in 1 M KOH; iii) the specific conductivity and selectivity are similar to those recently reported in the literature as the state of the art for AEM with potential application to alkaline DMFC; iv) the selectivity is a factor 2 higher than Nafion 117, and a factor between 5 and 10 times higher than membranes prepared with commercial QPAES.

The performance tests for the passive single fuel cell at room temperature are promising, considering that the use of a bimetallic anodic catalyst and a thinner membrane, to reduce the ohmic drop at the membrane, would increase its power density to values close to the state of the art for passive alkaline direct methanol fuel cells.

Unlike the observed for Nafion membranes, water uptake in QPAES is similar for massive and ultra-thin membranes, probably because the QPAES microstructure is not modified. This is relevant for the application of QPAES as AEM in alkaline DMFC, because the use of QPAES as a binder in the preparation of the membrane-electrode assemblies, will lead to AEM thin films in the three-phase region with similar characteristics to that of the bulky membrane.

Acknowledgments

The authors acknowledge MINCYT/NRF Cooperation Program RSA-Argentina (Grant 67370), ANPCyT (PICT 2091), and Consejo Nacional de Investigaciones Científicas y Técnicas (PIP 0095) for financial support. MM and PN thanks CSIR (MSM) for support. HRC is a member of Consejo Nacional de Investigaciones Científicas y Técnicas (CONICET). EAF thanks a fellowship by CONICET.

References

- [1] G. Olah, A.A. Goepfert, G.K. Surya Prakash, *Beyond Oil and Gas: the Methanol Economy*, Wiley-VCH Verlag, Weinheim, 2006.
- [2] T.S. Zhao, W.W. Yang, R. Chen, Q.X. Wu, *J. Power Sources* 195 (2010) 3451–3462.
- [3] P. Agnolucci, *Int. J. Hydrogen Energy* 32 (2007) 4319–4328.
- [4] X. Ren, T. Springer, T.A. Zawodzinski, S. Gottesfeld, *J. Electrochem. Soc.* 147 (2000) 466–474.
- [5] H.A. Every, M.A. Hickner, J.E. McGrath, T.A. Zawodzinski, *J. Membr. Sci.* 250 (2005) 183–188.
- [6] K. Ramya, K.S. Dhathathreyan, *J. Membr. Sci.* 311 (2008) 121–127.
- [7] S. Xue, G. Yin, K. Cai, Y. Shao, *J. Membr. Sci.* 289 (2007) 51–57.
- [8] L.A. Diaz, G.C. Abuin, H.R. Corti, *J. Membr. Sci.* 411 (2012) 35–44.
- [9] J.R. Varcoe, R.C.T. Slade, *Fuel Cells* 5 (2005) 187–200.
- [10] E.H. Yu, K. Scott, *J. Power Sources* 137 (2004) 248–256.
- [11] T. Schultz, S. Zhou, K. Sundmacher, *Chem. Eng. Technol.* 24 (2001) 1223–1233.
- [12] G.C. Abuin, P. Nonjola, E.A. Franceschini, F. Izraelevitch, M.K. Mathe, H.R. Corti, *Int. J. Hydrogen Energy* 35 (2010) 5849–5854.
- [13] A.V. Tripkovic, K.D. Popovic, B.N. Grgur, B. Blizanac, P.N. Ross, N.M. Markovic, *Electrochim. Acta* 47 (2002) 3707–3714.
- [14] E. Antolini, E.R. Gonzalez, *J. Power Sources* 195 (2010) 3431–3450.
- [15] K. Scott, E. Yu, *J. Power Sources* 175 (2008) 452–457.
- [16] J. Fang, P.K. Shen, *J. Membr. Sci.* 285 (2006) 317–322.
- [17] J. Hnat, M. Paidar, J. Schauer, J. Zitka, K. Bouzek, *J. Appl. Electrochem* 41 (2011) 1043–1052.
- [18] J.R. Varcoe, *Phys. Chem. Chem. Phys.* 9 (2007) 1479–1486.
- [19] G. Couture, A. Alaaeddine, F. Boschet, B. Ameduri, *Prog. Polym. Sci.* 36 (2011) 1521–1557.
- [20] E.H. Yu, U. Krewer, K. Scott, *Energies* 3 (2010) 1499–1528.
- [21] H.R. Corti, in: H.R. Corti, E.R. Gonzalez (Eds.), *Direct Alcohol Fuel Cells: Materials, Performance, Durability and Applications*, Springer, Dordrecht, 2014, pp. 121–230.
- [22] J.R. Varcoe, R.C.T. Slade, *Electrochem. Commun.* 8 (2006) 839–843.
- [23] L. Li, Y. Wang, *J. Membr. Sci.* 262 (2005) 1–4.
- [24] Y. Xiong, Q.L. Liu, Q.H. Zeng, *J. Power Sources* 193 (2009) 541–546.
- [25] C.H. Zhao, Y. Gong, Q.L. Liu, Q.G. Zhang, A.M. Zhu, *Int. J. Hydrogen Energy* 37 (2012) 11383–11393.
- [26] A.H.N. Rao, R.L. Thankamony, H.-J. Kim, S. Namb, T.-H. Kim, *Polymer* 54 (2013) 111–119.
- [27] Q. Zhang, Q. Zhang, J. Wang, S. Zhang, S. Li, *Polymer* 51 (2010) 5407–5416.
- [28] H. Jung, K. Fujii, T. Tamaki, H. Ohashi, T. Ito, T. Yamaguchi, *J. Membr. Sci.* 373 (2011) 107–111.
- [29] X. Li, Y. Yu, Y. Meng, *ACS Appl. Mater. Interfaces* 5 (2013) 1414–1422.
- [30] X. Li, Y. Yu, Q. Liu, Y. Meng, *ACS Appl. Mater. Interfaces* 4 (2012) 3627–3635.
- [31] G. Liu, Y. Shang, X. Xie, S. Wang, J. Wang, Y. Wang, Z. Mao, *Int. J. Hydrogen Energy* 37 (2012) 848–853.
- [32] Q.H. Zeng, Q.L. Liu, I. Broadwell, A.M. Zhu, Y. Xiong, X.P. Tu, *J. Membr. Sci.* 349 (2010) 237–243.
- [33] Y. Xiong, J. Fang, Q.H. Zeng, Q.L. Liu, *J. Membr. Sci.* 311 (2008) 319–325.
- [34] J. Hu, C. Zhang, J. Cong, H. Toyoda, M. Nagatsu, Y. Meng, *J. Power Sources* 196 (2011) 4483–4490.
- [35] C. Zhang, J. Hu, J. Cong, Y. Zhao, W. Shen, H. Toyoda, M. Nagatsu, Y. Meng, *J. Power Sources* 196 (2011) 5386–5393.
- [36] B.-S. Ko, Y.-J. Sohn, J. Shin, *Polymer* 53 (2012) 4652–4661.
- [37] C.C. Yang, S.J. Chiu, W.C. Chien, *J. Power Sources* 162 (2006) 21–29.
- [38] Y. Xiong, Q.L. Liu, A.M. Zhu, S.M. Huang, Q.H. Zeng, *J. Power Sources* 186

- (2009) 328–333.
- [39] C.C. Yang, S.S. Chiu, S.C. Kuo, T.H. Liou, J. Power Sources 199 (2012) 37–45.
- [40] C.C. Yang, S.J. Chiu, W.C. Chien, S.S. Chiu, J. Power Sources 195 (2010) 2212–2219.
- [41] Y. Xiong, Q.L. Liu, Q.G. Zhang, A.M. Zhu, J. Power Sources 183 (2008) 447–453.
- [42] J.M. Yang, H.C. Chiu, J. Membr. Sci. 419–420 (2012) 65–71.
- [43] C.C. Yang, J. Appl. Electrochem 42 (2012) 305–317.
- [44] K. Matsuoka, Y. Iriyama, T. Abe, M. Matsuoka, Z. Ogumi, J. Power Sources 150 (2005) 27–31.
- [45] N. Fujiwara, Z. Siroma, S. Yamazaki, T. Ioroi, H. Senoh, K. Yasuda, J. Power Sources 185 (2008) 621–626.
- [46] G.K.S. Prakash, F.C. Krause, F.A. Viva, S.R. Narayanan, G.A. Olah, J. Power Sources 196 (2011) 7967–7972.
- [47] J.H. Kim, H.K. Kim, K.T. Hwang, J.Y. Lee, Int. J. Hydrogen Energy 35 (2010) 768–773.
- [48] Y.S. Li, T.S. Zhao, Z.X. Liang, J. Power Sources 187 (2009) 387–392.
- [49] E.H. Yu, K. Scott, R.W. Reeve, J. Appl. Electrochem 36 (2006) 25–32.
- [50] C. Coutanceau, L. Demarconnay, C. Lamy, J.M. Léger, J. Power Sources 156 (2006) 14–19.
- [51] E.H. Yu, K. Scott, J. Appl. Electrochem 35 (2005) 91–96.
- [52] K. Scott, E.H. Yu, G. Vlachogiannopoulos, M. Shivare, N. Duteanu, J. Power Sources 175 (2008) 452–457.
- [53] A. Santasalo-Aarnio, S. Hietala, T. Rauhala, T. Kallio, J. Power Sources 196 (2011) 6153–6159.
- [54] P.V. Mazin, N.A. Kapustina, M.R. Tarasevich, Russ. J. Electrochem 47 (2011) 275–281.
- [55] G.M. Geise, M.A. Hickner, B.E. Logan, ACS Appl. Mater. Interfaces 5 (2013) 10294–10301.
- [56] J. Wang, J. Wang, S. Li, S. Zhang, J. Membr. Sci. 368 (2011) 246–253.
- [57] Y. Leng, G. Chen, A.J. Mendoza, T.B. Tighe, M.A. Hickner, J. Am. Chem. Soc. 134 (2012) 9054–9057.
- [58] L.H. Sperling, Introduction to Physical Polymer Science, second ed., John Wiley & Sons, New York, 1992.
- [59] G.C. Abuin, M.C. Fuertes, H.R. Corti, J. Membr. Sci. 428 (2013) 507–515.
- [60] H. Hertz, J. Reine Angew. Math. 92 (1882) 156–171.
- [61] E.A. Franceschini, H.R. Corti, J. Power Sources 188 (2009) 379–386.
- [62] C. Wang, Y. Weng, D. Chu, R. Chen, D. Xie, J. Membr. Sci. 332 (2009) 63–68.
- [63] D. Rivin, C.E. Kendrick, P.W. Gibson, N.S. Schneider, Polymer 42 (2001) 623–635.
- [64] Y. Tang, A.M. Karlsson, A.M. Santare, M. Gilbert, S. Cleghorn, W.B. Johnson, Mat. Sci. Eng. A 425 (2006) 297–304.
- [65] S. Ates, C. Dizman, B. Aydogan, B. Kiskan, L. Torun, Y. Yagci, Polymer 52 (2011) 1504–1509.
- [66] M.L. Di Vona, E. Sgreccia, M. Tamilvanan, M. Khadhraoui, C. Chassigneux, P. Knauth, J. Membr. Sci. 354 (2010) 134–141.
- [67] Y. Huang, C. Xiao, Polymer 48 (2007) 371–381.
- [68] B.S. Pivovar, Y. Wang, E.L. Cussler, J. Membr. Sci. 154 (1999) 155–162.
- [69] A.H.N. Rao, H.-J. Kim, S. Nam, T.-H. Kim, Polymer 54 (2013) 6918–6928.
- [70] Z. Wei, S. He, X. Liu, J. Qiao, J. Lin, L. Zhang, Polymer 54 (2013) 1243–1250.